

# Bio-Inspired Stable Lithium-Metal Anodes by Co-depositing Lithium with a 2D Vermiculite Shuttle

Qingtao Ma<sup>+</sup>, Xiaowen Sun<sup>+</sup>, Ping Liu, Yongyao Xia, Xingjiang Liu, and Jiayan Luo\*

**Abstract:** Progress in lithium-metal batteries is severely hindered by lithium dendrite growth. Lithium is soft with a mechanical modulus as low as that of polymers. Herein we suppress lithium dendrites by forming soft–hard organic–inorganic lamella reminiscent of the natural sea-shell material nacre. We use lithium as the soft segment and colloidal vermiculite sheets as the hard inorganic constituent. The vermiculite sheets are highly negatively charged so can absorb  $\text{Li}^+$  then be co-deposited with lithium, flattening the lithium growth which remains dendrite-free over hundreds of cycles. After  $\text{Li}^+$  ions absorbed on the vermiculite are transferred to the lithium substrate, the vermiculite sheets become negative charged again and move away from the substrate along the electric field, allowing them to absorb new  $\text{Li}^+$  and shuttling to and from the substrate. Long term cycling of full cells using the nacre-mimetic lithium-metal anodes is also demonstrated.

**L**ithium-metal batteries (LMBs), containing lithium-sulfur and lithium-air, recently began to flourish for energy storage with high energy density.<sup>[1]</sup> The performance of lithium metal batteries is largely determined by the plating morphology of lithium.<sup>[2]</sup> Uneven lithium deposition results in proliferative lithium dendrites that grow fastest at the apex.<sup>[3]</sup> The lithium dendrites with their large surface area and aspect ratio can cause various side reactions with the electrolyte, forming an unstable solid electrolyte interphase (SEI) which is easily broken during Li plating/stripping, further resulting in a large number of unfavorable changes to the lithium morphology.<sup>[4]</sup> In addition, a series of problems, such as structural pulverization and volume expansion during deposition and dissolution may also occur. Therefore, the morphological transformation of lithium deposition is the dominant reason behind poor Columbic efficiency, short cycle life, and safety hazards in

lithium-metal batteries.<sup>[5]</sup> Many strategies have been developed to address the dendrite issues,<sup>[6]</sup> such as modification of the separator,<sup>[7]</sup> synthesis of the solid electrolyte,<sup>[8]</sup> confining lithium in local space,<sup>[9]</sup> and structured anodes.<sup>[10]</sup>

Nacres, also known as mother of pearl, has a unique soft-hard organic–inorganic composite lamella structure (Figure 1 a,b).<sup>[11]</sup> The organic matter is bonded to the inorganic ceramics through a series of interactions. During the fracture process, the organic layers preferentially plastically deform to act as a buffer zone and hinder crack propagation of the ceramics.<sup>[12]</sup> The unique soft-hard alternating assembled structure show exceptional highly ordered growth, high tensile strengths, hardness, toughness, and dense structures, which have stimulated the design and manufacture of a myriad of functional materials. Moreover, during the brick-laying assembling process, the nucleation and growth of nacre is well controlled through the molecular level interaction of organic molecules and inorganic ions.<sup>[13]</sup> Such a mechanism can be applied into Li metal anodes as well. Clay is often utilized as an inorganic material owing to its negative charge, large two-dimensional structure, and high Young's modulus. Kotov et al. prepared a series of shell structured materials using a clay/polymer by layer-by-layer method.<sup>[14]</sup> The negatively charged clay flakes and the positively charged polyelectrolytes were alternately adsorbed together to form a highly ordered stacked layer structure. Consequently, it seems reasonable to design a nacre-mimetic Li metal anode using clay as the inorganic rigid segment.

Polymers have a Young's modulus of 0.4–4.83 Gpa and ceramics have much higher Young's modulus of 64–413 Gpa (Figure 1 c).<sup>[15]</sup> Metals have a wider modulus range that lies between that of polymers and ceramics. The Young's modulus of lithium metal is only 4.9 Gpa, which is as low as polymers.<sup>[16]</sup> Thus we were inspired to design nacre-like lithium metal anodes in which the lithium acts like the soft organic segment to coordinate with clay. In our earlier study, the mechanical modulus of poly(ethylene oxide) was enhanced by incorporating vermiculite sheets (VS).<sup>[17]</sup> Vermiculite is a layered clay material with theoretical Young's modulus of 170 Gpa (Figure 1 c)<sup>[18]</sup> and can be exfoliated to single sheets. The vermiculite sheet film fabricated by restacking of sheets has a practical Young's modulus as high as 47 Gpa, which is an order of magnitude higher than that of lithium (Figure 1 d). Thus vermiculite sheets can serve as the hard building block for the soft-hard alternating structure. Herein we show an innovative bio-inspired strategy to address the lithium dendrite problem. The vermiculite sheet as the rigid inorganic substance can co-deposit during the plating of the soft Li segment and form a rock-like dense morphology,

[\*] Q. Ma,<sup>[†]</sup> X. Sun,<sup>[†]</sup> Prof. X. Liu, Prof. J. Luo  
Key Laboratory for Green Chemical Technology of Ministry of Education, State Key Laboratory of Chemical Engineering, School of Chemical Engineering and Technology, Tianjin University  
Tianjin 300072 (China)  
E-mail: jluo@tju.edu.cn

Prof. P. Liu  
Department of NanoEngineering, University of California San Diego  
La Jolla, CA 92093 (USA)

Prof. Y. Xia  
Department of Chemistry, Institute of New Energy, Fudan University  
Shanghai 200433 (China)

[†] These authors contributed equally to this work.

Supporting information and the ORCID identification number(s) for the author(s) of this article can be found under:  
<https://doi.org/10.1002/anie.201900783>.

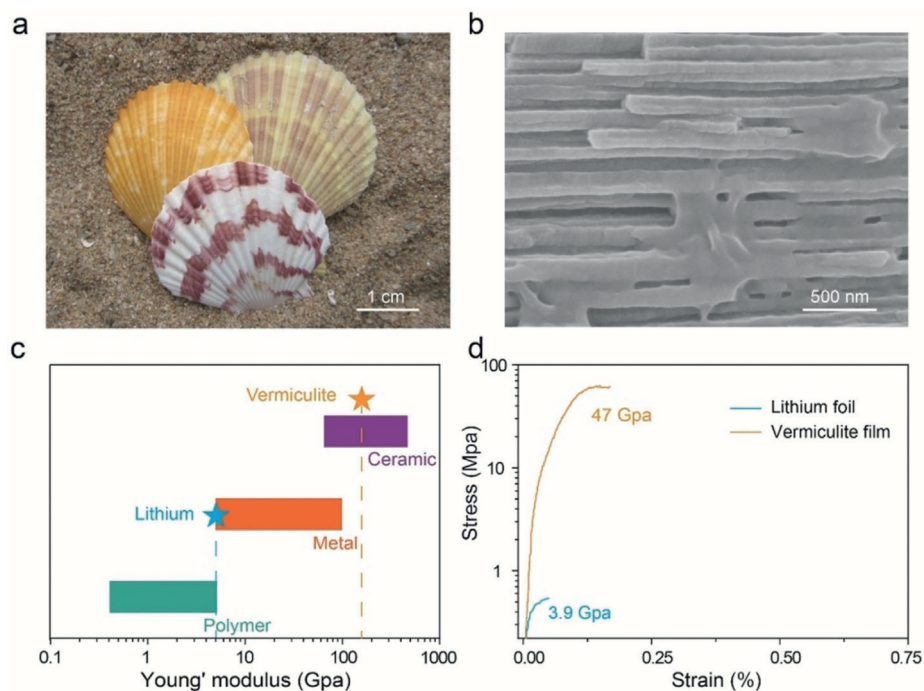


**Figure 1.** Nacre-inspired Li metal anode design. a) Photograph of shells. b) Cross-sectional SEM image of nacre. c) Young's modulus of polymers, metals, ceramics, lithium and vermiculite. d) Stress-strain curves of the lithium foil and vermiculite sheets.

which significantly improves the long-cycling electrochemical performance of lithium metal anodes.

Vermiculite sheets consist of two layers of silicon oxygen tetrahedra and one layer of magnesium octahedra (Figure 2a). The  $\text{Si}^{4+}$  of the silicon tetrahedron is partially replaced by  $\text{Al}^{3+}$  which makes the sheets negatively charged. The layers of vermiculite are held together by weak hydrogen bonds and van der Waals forces so the layers are readily exfoliated to single or few layered sheets,<sup>[19]</sup> as shown in the X-ray diffraction (XRD) patterns and scanning electron microscopy (SEM) image (Figure S1 in the Supporting Information). The thickness of a bilayer is 3 nm and the lateral size is on the micrometer scale (Figure 2b). Vermiculite sheets could be well dispersed in water with the zeta potential around  $-34$  mV at different concentrations (Figure 2c). When 1M LiCl was added to the aqueous dispersion, the zeta potential dropped to  $-10$  mV confirming  $\text{Li}^+$  can be absorbed on the surface of vermiculite sheet. Owing to the

substantial negative charge, the vermiculite sheet can also be colloiddally dispersed in carbonate electrolytes without any treatment (Figure S2). Note, the vermiculite sheet are inert in broad electrochemical window. Identical curves were obtained through cyclic voltammetry tests of  $\text{Li}||\text{Cu}$  cells in electrolytes with and without vermiculite sheet additive, which confirms the stability of vermiculite sheet during Li plating/stripping (Figure S3).

In carbonate-based electrolyte, Li deposited at a current density of  $0.1 \text{ mA cm}^{-2}$  shows typical dendritic structure with diameter of  $100\text{--}200 \text{ nm}$  (Figure S4 a,b).<sup>[20]</sup> The Li deposition was fluffy and uneven. However, a dense structure of deposited Li with a smooth surface was observed in ethylene carbonate (EC)/ diethyl carbonate (DEC) (1:1 by volume) electrolyte with the vermiculite sheet additive (Figure S4 c,d). By monitoring the initial nucleation stage at low Li deposition, Li was found to nucleate sporadically with irregular shapes in the vermiculite-sheet-free electrolyte, while large

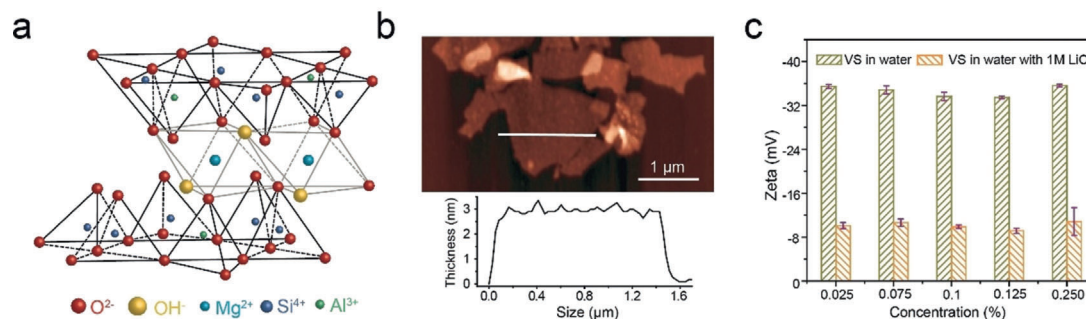


**Figure 2.** Characteristics of vermiculite sheets. a) Crystal structure of vermiculite. b) Atomic force microscopy (AFM) image and the corresponding height profile of exfoliated vermiculite sheet. c) Zeta potential of vermiculite sheet in water and 1 M LiCl aqueous solution at different concentrations.

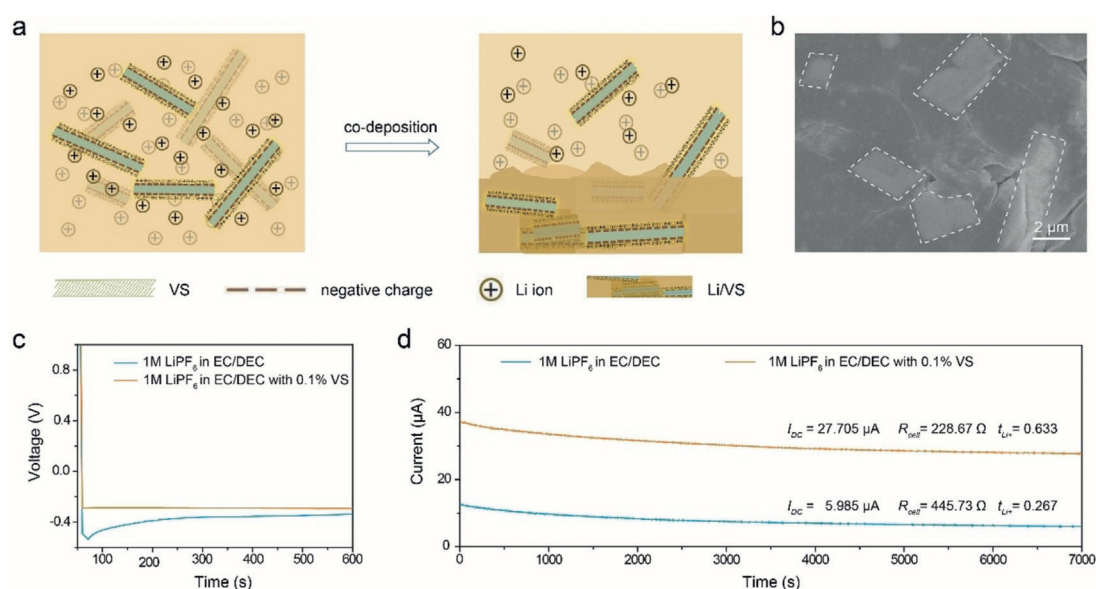


**Figure 3.** a) Schematic illustrating the co-deposition of Li with vermiculite sheet. b) BSE image of Li plating in EC/DEC electrolyte with 0.1% vermiculite sheet. c) The voltage–time curves during Li nucleation at  $0.5 \text{ mA cm}^{-2}$  on Cu substrates. d) Chronoamperogram of LiPF<sub>6</sub> EC/DEC electrolyte with and without vermiculite sheets under an applied voltage of 10 mV.

flake shaped deposits were obtained in the electrolyte containing vermiculite sheets (Figure S5). This difference may be ascribed to the co-deposition of vermiculite sheets and Li in the electrolyte containing vermiculite-sheets and the unique nacre-like structure of the Li metal anode during cycling. At a higher current density of  $0.5 \text{ mA cm}^{-2}$ , a dendrite-free flake-like morphology was still observed in the electrolyte containing vermiculite sheets (Figure S6). Better plating quality, higher Coulombic efficiency and lower resistance of Li plating/stripping on Cu foil were found in the vermiculite sheet containing electrolyte than in the electrolyte without vermiculite sheet (Figure S7, S8).

Figure 3a shows how the vermiculite sheet participated in Li deposition. First, the negative charged vermiculite sheet absorb plenty of Li<sup>+</sup> from the electrolyte onto their surfaces by electrostatic force, increasing the local Li<sup>+</sup> concentration. Then, the vermiculite sheets co-deposit on the current collectors with the absorbed Li<sup>+</sup>, leading to flake-like Li nucleation. The co-deposited vermiculite sheets can serve as flat substrates for further Li deposition. They can also flatten the already deposited Li due to their two-dimensional structure and high Young's modulus. These properties collectively suppress the Li dendrite growth. Indeed, unfolded vermiculite sheets are present in the deposited Li as observed from the backscattered electron (BSE) image which gives evidence to the co-depositing mechanism (Figure 3b). To validate the co-deposition of vermiculite sheet and Li, energy dispersive X-ray spectroscopy (EDX) mapping and X-ray photoelectron spectroscopy (XPS) characterizations were conducted. Si signal was conspicuously observed from the deposited Li through EDX mapping, indicating the vermiculite sheet participated in whole Li plating progress (Figure S9). XPS survey of the deposited Li also shows the signal of the Si 2p and Mg 2s thus further demonstrating the co-

deposition of vermiculite sheet and Li<sup>+</sup> during Li plating (Figure S10).<sup>[21]</sup>

According to Chazalviel's model,<sup>[22]</sup> Li dendrite growth is controlled by concentration variation and Sand's time<sup>[4b]</sup>. The laminated structure of vermiculite can guide the lateral Li<sup>+</sup> diffusion to control the Li nucleation and deposition, and meanwhile the vermiculite sheets can replenish Li<sup>+</sup> by their high ion absorbing capacity, which decreases the Li<sup>+</sup> concentration gradient in the vermiculite sheet containing colloidal electrolyte. As a result, the nucleation overpotential on the Cu substrate decreased significantly from 0.190 V to 0.006 V after adding the vermiculite sheets (Figure 3c). To further understand the migration of Li<sup>+</sup>, the Li<sup>+</sup> transference numbers ( $t_{Li^+}$ ) was calculated according to Equation (1)<sup>[5a]</sup>

$$t_{Li^+} = R_{cell}/R_{DC} \quad (1)$$

where  $R_{cell}$  is the total cell resistance,  $R_{DC} = V_{DC}/I_{DC}$ , which  $V_{DC}$  is the applied potential,  $I_{DC}$  is the steady-state current recorded in chronoamperometry (Figure 3d). The Li<sup>+</sup> transference number increase significantly from 0.267 to 0.633 after adding the vermiculite sheets.

To visualize the co-deposition of vermiculite and Li, the Li plating process was recorded under optical microscopy using Li||Li symmetric cell. In EC/DEC electrolyte, sparse particles appeared after applying a current density of  $2 \text{ mA cm}^{-2}$  for 20 seconds. These particles became huge "mossy" clusters after 60 seconds as the deposition capacity increased (Figure 4a, Video S1). A complete different phenomenon was observed in electrolyte with vermiculite sheets. Before the electric field was applied, colloidal Brownian motion of the vermiculite sheets was observed (Figure 4b, Video S2). At the same current density of  $2 \text{ mA cm}^{-2}$  as in vermiculite sheets free electrolyte, the vermiculite sheets moved towards the Li

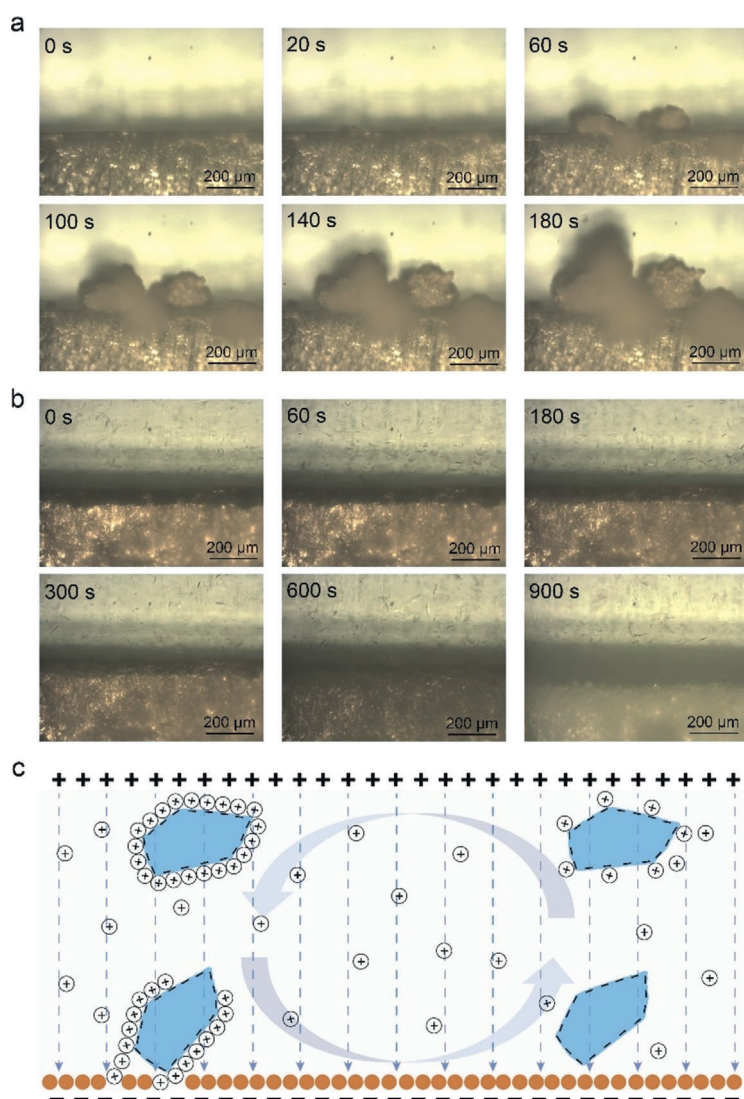


**Figure 4.** In situ optical microscopy observation of the shuttling effect of vermiculite sheets during Li deposition. Snapshots of optical microscopy images of Li deposited in a) 1 M LiPF<sub>6</sub> in EC/DEC electrolyte and b) 1 M LiPF<sub>6</sub> in EC/DEC with 0.1% vermiculite sheet containing electrolyte. c) Schematic representation of the shuttling effect of vermiculite sheets for homogeneous Li deposition.

substrate and co-deposited with Li plating. No cluster formation was observed even after 900 seconds, suggesting Li was homogeneously deposited on the substrate. Interestingly, movement of vermiculite sheets in the opposite direction away from the substrate was also observed. This is because once the Li<sup>+</sup> absorbed on the vermiculite sheets has been deposited on the substrate, the partially un-deposited vermiculite sheets became highly negative charged again and moved away from the substrate along the electric field (Figure 4c). These vermiculite sheets can further absorb and replenish new Li<sup>+</sup> for homogeneous deposition.

The voltage hysteresis of the symmetric cells in the EC/DEC electrolyte increased rapidly after 200 h cycling and failed after 290 h at current density of 1 mA cm<sup>-2</sup> (see Figure 5a). While the voltage hysteresis in the EC/DEC electrolyte containing 0.1% vermiculite sheets was much

smaller and maintained stable even after 600 h. When increasing the current density to 2 mA cm<sup>-2</sup>, the cells in EC/DEC electrolyte containing 0.1% vermiculite sheets can be cycled over 250 h, which greatly surpassed the cells in VS the electrolyte without vermiculite sheets (see Figure 5b, Figure S11). The symmetric cells also showed better performance in the vermiculite sheets containing ether electrolyte than in pure ether electrolyte (Figure S12). Such exceptional cycling performance is a good indicator of the superiority of the nacre-like anode. As a proof of concept, Li||LiFePO<sub>4</sub> (LFP) full cells were assembled using two different electrolytes. The Li||LFP battery underwent a capacity drop after only 65 cycles at 0.5 C (1.0 C = 170 mAh g<sup>-1</sup>) in EC/DEC electrolyte (see Figure 5c, Figure S13). In contrast, the capacity maintained 130.4 mAh g<sup>-1</sup> over 150 cycles with a fading rate as low as 0.034% per cycle in the EC/DEC electrolyte with 0.1% vermiculite sheets. To investigate the reason for the capacity fading, we compared the morphology of Li anode after different cycles (see Figure 5d–i). Dendritic lithium appeared at the first plating cycle in EC/DEC electrolyte (Figure 5d), and then evolved to a porous structure after 10 cycles (Figure 5e). Obvious fractures were observed after 40 cycles (Figure 5f). The coarse and fractured structure resulted in unstable SEI and “dead” lithium, which led to continuous decay of the Coulombic efficiency even the capacity was stable at the initial cycles. However, the Li deposited with vermiculite sheets always maintained a dense structure with a smooth surface and remained dendrite and fracture free after cycling thus demonstrating the effectiveness of the biomimetic strategy (Figure 5g–i).

In conclusion, the bio-inspired design of nacre-like lithium metal anodes takes advantage of the low Young's modulus of soft lithium. The high Young's modulus, high negative charge, and two dimensional structure make vermiculite sheets the ideal hard building block for the soft-hard alternating nacre-like structure. We co-deposited the lithium-vermiculite composite by adding vermiculite into the EC/DEC electrolyte. The nacre-mimetic lithium metal anodes are dendrite-free over hundreds of cycles. Other 2D materials with different functionalities could be used or developed for high performance lithium metal anodes. This bio-inspired approach may lead to unconventional strategies to address the dendrite problems of lithium and other metal anodes.

### Acknowledgements

We appreciate support from National Natural Science Foundation of China (Grant Nos. 51872196, U1601206), Natural Science Foundation of Tianjin, China (Grant Nos. 17JCQJC44100) and Metal Fuel Cell Key Laboratory of Sichuan Province.

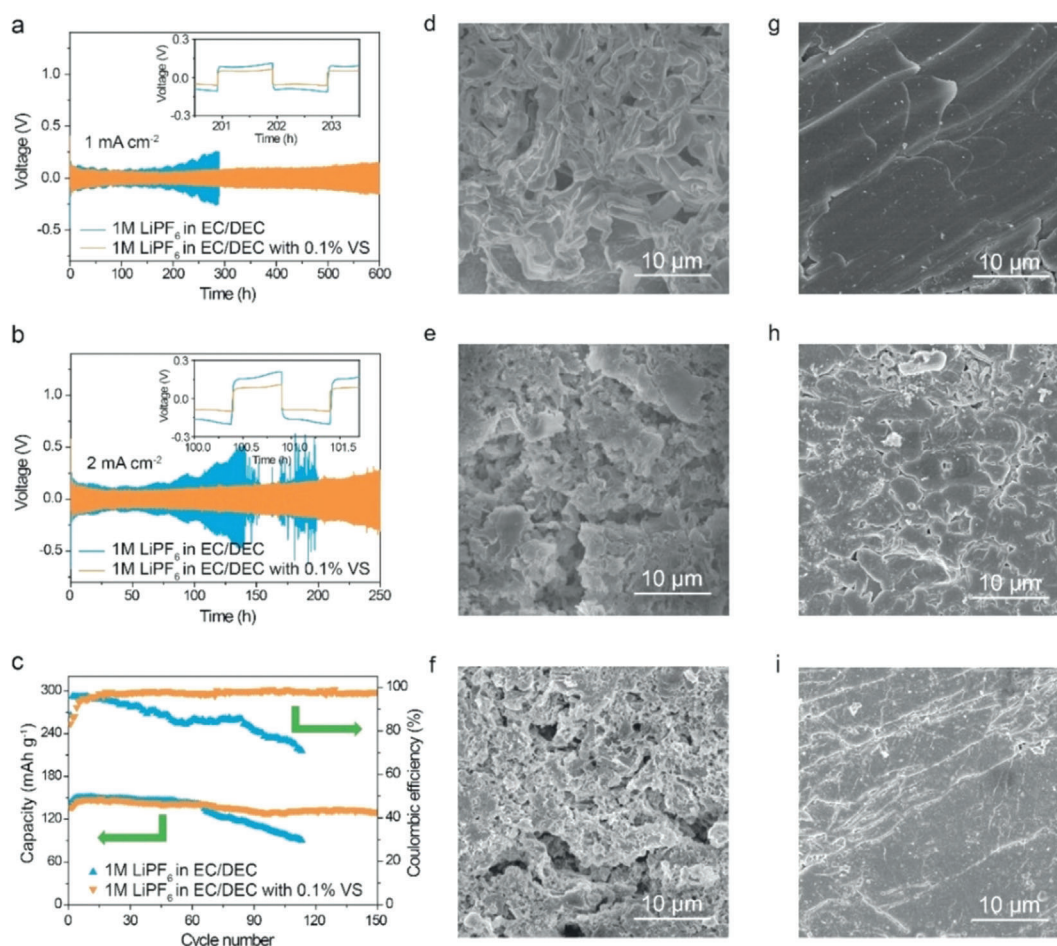


**Figure 5.** Cycling performance of symmetric cells under a)  $1 \text{ mA cm}^{-2}$ , b)  $2 \text{ mA cm}^{-2}$  with the capacity at  $1 \text{ mAh cm}^{-2}$ . Inset: the Li plating/stripping voltage profiles. c) Cycling performance of Li | LFP full cell at  $0.5 \text{ C}$ . SEM images of Li after d) 1, e) 10, f) 40 plating/stripping cycles in EC/DEC electrolyte and after g) 1, h) 10, i) 40 cycles in EC/DEC electrolyte with 0.1% vermiculite sheets.

### Conflict of interest

The authors declare no conflict of interest.

**Keywords:** bioinspired materials · dendrite suppression · electrode materials · lithium-metal anodes · vermiculite

- [1] a) P. G. Bruce, S. A. Freunberger, L. J. Hardwick, J.-M. Tarascon, *Nat. Mater.* **2012**, *11*, 19; b) A. Wang, S. Tang, D. Kong, S. Liu, K. Chiou, L. Zhi, J. Huang, Y. Y. Xia, J. Luo, *Adv. Mater.* **2018**, *30*, 1703891; c) D. Lei, K. Shi, H. Ye, Z. Wan, Y. Wang, L. Shen, B. Li, Q.-H. Yang, F. Kang, Y.-B. He, *Adv. Funct. Mater.* **2018**, *28*, 1707570.
- [2] L. Li, S. Basu, Y. Wang, Z. Chen, P. Hundekar, B. Wang, J. Shi, Y. Shi, S. Narayanan, N. Koratkar, *Science* **2018**, *359*, 1513.
- [3] a) X.-B. Cheng, R. Zhang, C.-Z. Zhao, Q. Zhang, *Chem. Rev.* **2017**, *117*, 10403; b) X. Fan, L. Chen, X. Ji, T. Deng, S. Hou, J. Chen, J. Zheng, F. Wang, J. Jiang, K. Xu, *Chem* **2018**, *4*, 174; c) Q. Yun, Y.-B. He, W. Lv, Y. Zhao, B. Li, F. Kang, Q.-H. Yang, *Adv. Mater.* **2016**, *28*, 6932.
- [4] a) D. Lin, Y. Liu, Y. Cui, *Nat. Nanotechnol.* **2017**, *12*, 194; b) W. Xu, J. Wang, F. Ding, X. Chen, E. Nasybulin, Y. Zhang, J.-G. Zhang, *Energy Environ. Sci.* **2014**, *7*, 513.

- [5] a) L. Suo, Y.-S. Hu, H. Li, M. Armand, L. Chen, *Nat. Commun.* **2013**, *4*, 1481; b) R. Mukherjee, A. V. Thomas, D. Datta, E. Singh, J. Li, O. Eksik, V. B. Shenoy, N. Koratkar, *Nat. Commun.* **2014**, *5*, 3710.
- [6] a) S. Liu, A. Wang, Q. Li, J. Wu, K. Chiou, J. Huang, J. Luo, *Joule* **2018**, *2*, 184; b) F. Ding, W. Xu, G. L. Graff, J. Zhang, M. L. Sushko, X. Chen, Y. Shao, M. H. Engelhard, Z. Nie, J. Xiao, *J. Am. Chem. Soc.* **2013**, *135*, 4450; c) Y. Gao, Y. Zhao, Y. C. Li, Q. Huang, T. E. Mallouk, D. Wang, *J. Am. Chem. Soc.* **2017**, *139*, 15288; d) Y. Gu, W.-W. Wang, Y.-J. Li, Q.-H. Wu, S. Tang, J.-W. Yan, M.-S. Zheng, D.-Y. Wu, C.-H. Fan, W.-Q. Hu, *Nat. Commun.* **2018**, *9*, 1339; e) C. Zhang, S. Liu, G. Li, C. Zhang, X. Liu, J. Luo, *Adv. Mater.* **2018**, *30*, 1801328; f) C. Yan, X. B. Cheng, Y. X. Yao, X. Shen, B. Q. Li, W. J. Li, R. Zhang, J. Q. Huang, H. Li, Q. Zhang, *Adv. Mater.* **2018**, *30*, 1804461.
- [7] a) W. Luo, L. Zhou, K. Fu, Z. Yang, J. Wan, M. Manno, Y. Yao, H. Zhu, B. Yang, L. Hu, *Nano Lett.* **2015**, *15*, 6149; b) Y. Qiao, Y. He, S. Wu, K. Jiang, X. Li, S. Guo, P. He, H. Zhou, *ACS Energy Lett.* **2018**, *3*, 463; c) Y. Liu, Q. Liu, L. Xin, Y. Liu, F. Yang, E. A. Stach, J. Xie, *Nat. Energy* **2017**, *2*, 17083.
- [8] a) Y. Li, H. Xu, P. H. Chien, N. Wu, S. Xin, L. Xue, K. Park, Y. Y. Hu, J. B. Goodenough, *Angew. Chem. Int. Ed.* **2018**, *57*, 8587; *Angew. Chem.* **2018**, *130*, 8723; b) N. W. Li, Y. X. Yin, C. P. Yang, Y. G. Guo, *Adv. Mater.* **2016**, *28*, 1853; c) Z. Wan, et al., *Adv. Funct. Mater.* **2019**, *29*, 1805301.
- [9] a) G. Zheng, S. W. Lee, Z. Liang, H.-W. Lee, K. Yan, H. Yao, H. Wang, W. Li, S. Chu, Y. Cui, *Nat. Nanotechnol.* **2014**, *9*, 618; b) A.

- Wang, X. Zhang, Y.-W. Yang, J. Huang, X. Liu, J. Luo, *Chem* **2018**, *4*, 2192; c) X. Zhang, R. Lv, A. Wang, W. Guo, X. Liu, J. Luo, *Angew. Chem. Int. Ed.* **2018**, *57*, 15028; *Angew. Chem.* **2018**, *130*, 15248.
- [10] Y. Liu, D. Lin, Z. Liang, J. Zhao, K. Yan, Y. Cui, *Nat. Commun.* **2016**, *7*, 10992.
- [11] a) S. Tadepalli, J. M. Slocik, M. K. Gupta, R. R. Naik, S. Singamaneni, *Chem. Rev.* **2017**, *117*, 12705; b) U. G. Wegst, H. Bai, E. Saiz, A. P. Tomsia, R. O. Ritchie, *Nat. Mater.* **2015**, *14*, 23.
- [12] H. Zhao, Z. Yang, L. Guo, *NPG Asia Mater.* **2018**, *10*, 1.
- [13] S. Mann, D. D. Archibald, J. M. Didymus, T. Douglas, B. R. Heywood, F. C. Meldrum, N. J. Reeves, *Science* **1993**, *261*, 1286.
- [14] Z. Tang, N. A. Kotov, S. Magonov, B. Ozturk, *Nat. Mater.* **2003**, *2*, 413.
- [15] M. F. Ashby, D. Cebon, *J. Phys. IV* **1993**, *3*, C6.
- [16] H. Tian, Z. W. Seh, K. Yan, Z. Fu, P. Tang, Y. Lu, R. Zhang, D. Legut, Y. Cui, Q. Zhang, *Adv. Energy Mater.* **2017**, *7*, 1602528.
- [17] W. Tang, S. Tang, C. Zhang, Q. Ma, Q. Xiang, Y. W. Yang, J. Luo, *Adv. Energy Mater.* **2018**, *8*, 1800866.
- [18] J. W. Suk, R. D. Piner, J. An, R. S. Ruoff, *Thin Solid Films* **2013**, *527*, 205.
- [19] G. Walker, W. Garrett, *Science* **1967**, *156*, 385.
- [20] F. Shi, A. Pei, A. Vailionis, J. Xie, B. Liu, J. Zhao, Y. Gong, Y. Cui, *Proc. Natl. Acad. Sci. USA* **2017**, *114*, 12138.
- [21] A. González-Elipe, J. Espinos, G. Munuera, J. Sanz, J. Serratos, *J. Phy. Chem.* **1988**, *92*, 3471.
- [22] J.-N. Chazalviel, *Phys. Rev. A* **1990**, *42*, 7355.

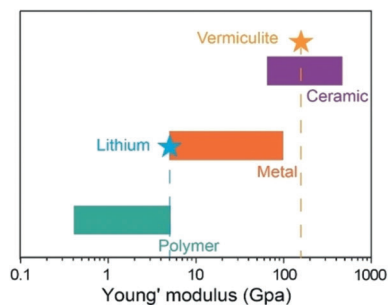
Manuscript received: January 20, 2019

Version of record online: ■■■■■■, ■■■■■■

## Communications

VIP

## Lithium-Metal Batteries

Q. Ma, X. Sun, P. Liu, Y. Xia, X. Liu,  
J. Luo\* ————— ■■■-■■■Bio-Inspired Stable Lithium-Metal  
Anodes by Co-depositing Lithium with  
a 2D Vermiculite Shuttle

A **soft–hard** organic–inorganic lamellar is constructed by using Li as the soft segment and colloidal vermiculite sheets as the hard constituent. The vermiculite sheets have a high negative charge so can absorb  $\text{Li}^+$  and deposit it on a lithium substrate, flattening the Li growth and forming a structure that is dendrite-free over hundreds of cycles for lithium-metal batteries.